The American Journal of Human Genetics, Volume *95*
Supplemental Data

Mutations in *GTPBP3* Cause a Mitochondrial Translation Defect Associated with Hypertrophic Cardiomyopathy, Lactic Acidosis, and Encephalopathy

Robert Kopajtich, Thomas J. Nicholls, Joanna Rorbach, Metodi D. Metodiev, Peter Freisinger, Hanna Mandel, Arnaud Vanlander, Daniele Ghezzi, Rosalba Carrozzo, Robert W. Taylor, Klaus Marquard, Kei Murayama, Thomas Wieland, Thomas Schwarzmayr, Johannes A. Mayr, Sarah F. Pearce, Christopher A. Powell, Ann Saada, Akira Ohtake, Federica Invernizzi, Eleonora Lamantea, Ewen W. Sommerville, Angela Pyle, Patrick F. Chinnery, Ellen Crushell, Yasushi Okazaki, Masakazu Kohda, Yoshihito Kishita, Yoshimi Tokuzawa, Zahra Assouline, Marlène Rio, François Feillet, Bénédict Mousson de Camaret, Dominique Chretien, Arnold Munnich, Björn Menten, Tom Sante, JoélSmet, Luc Régal, Abraham Lorber, Asaad Khoury, Massimo Zeviani, Tim M. Strom, Thomas Meitinger, Enrico S. Bertini, Rudy Van Coster, Thomas Klopstock, Agnès Rötig, Tobias B. Haack, Michal Minczuk, and Holger Prokisch

Figure S1

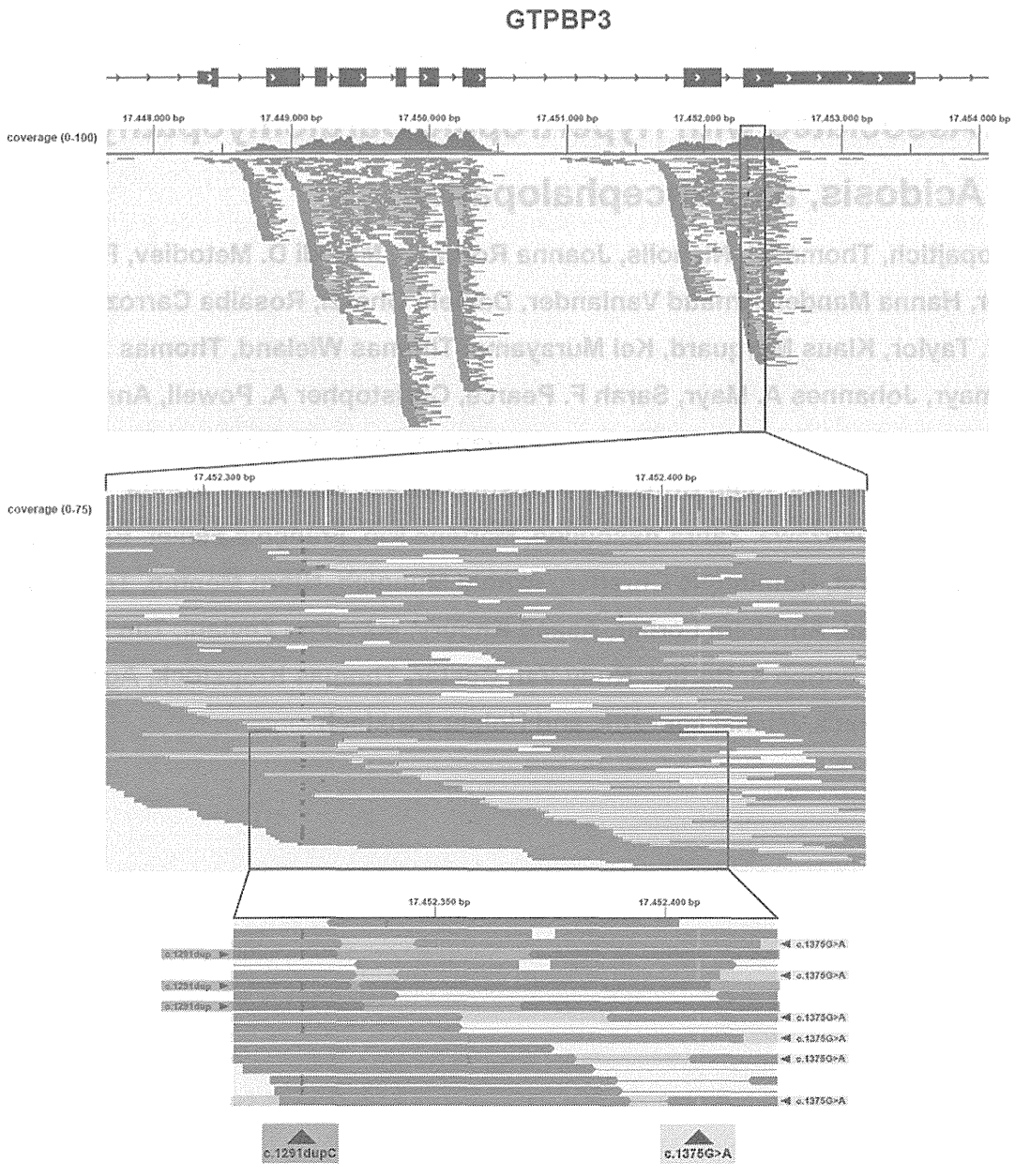

Figure S1) Segregation analysis in family F1 in WES data

The two mutations identified in family F1 (c.1291dupC and c.1375G>A) are only separated by 97 bp which allowed analysis of both alleles despite the lack of parental material. 13 paired sequence reads were identified which covered the region of both variants. All reads contained either of the two mutations demonstrating a compound heterozygous status of the two variants. Figure S1 shows three sequence reads containing the c.1291dupC variant and five reads containing the c.1375G>A variant.

Figure S2

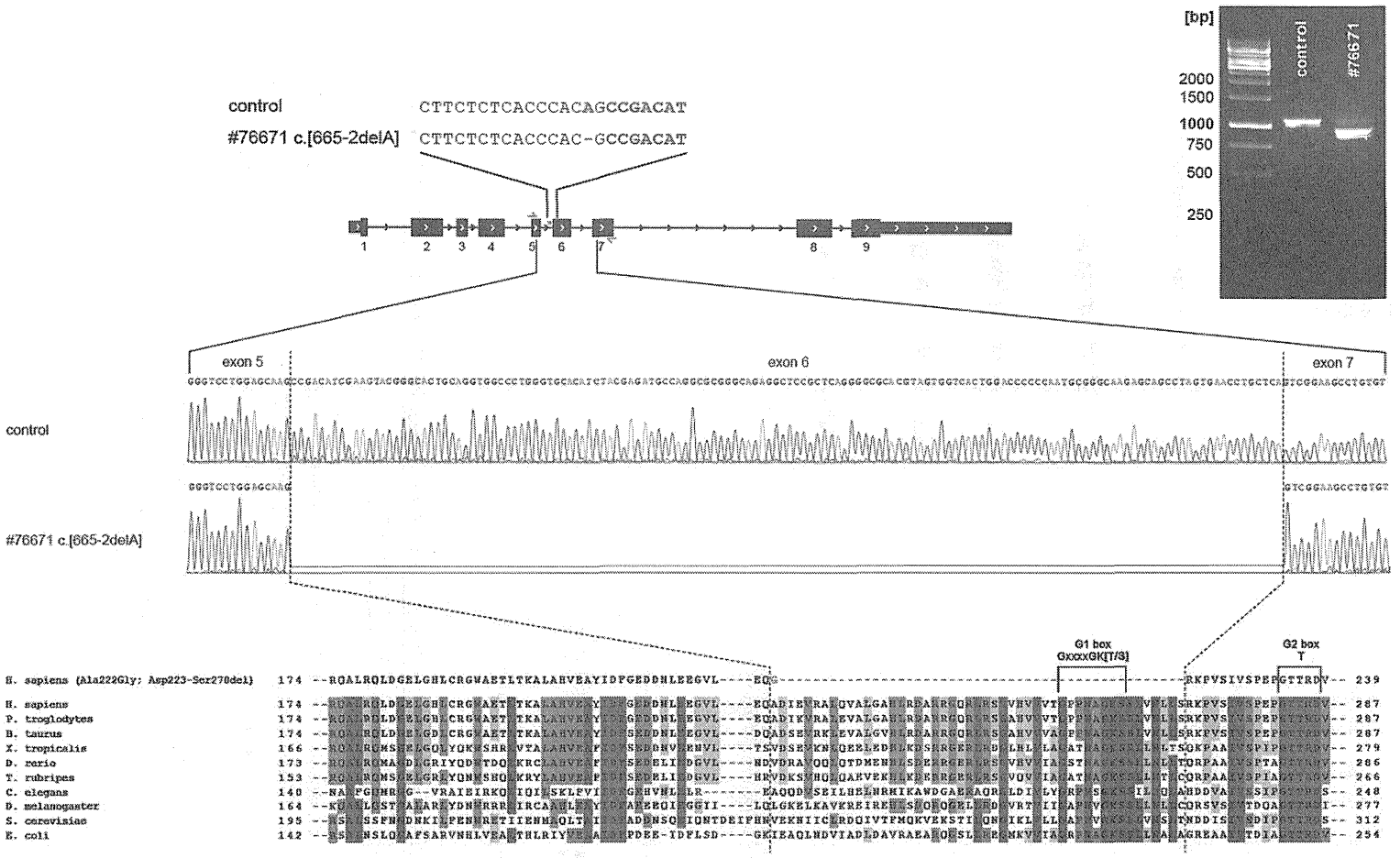

Figure S2) Splice site mutation in individual #76671 causes skipping of exon 6

Analysis of cDNA derived from fibroblasts of individual #76671 yielded a smaller than expected PCR product, indicating alternative splicing. Sanger sequencing revealed that the c.665-2delA mutation affects the conserved splice acceptor site. The splice acceptor upstream of exon 7 is alternatively used, yielding a mature mRNA that lacks exon 6. The resulting protein product is predicted to contain a 1 amino acid exchange followed by a 48 amino acid deletion (p.Ala322Gly; Asp223-270del).

Figure S3

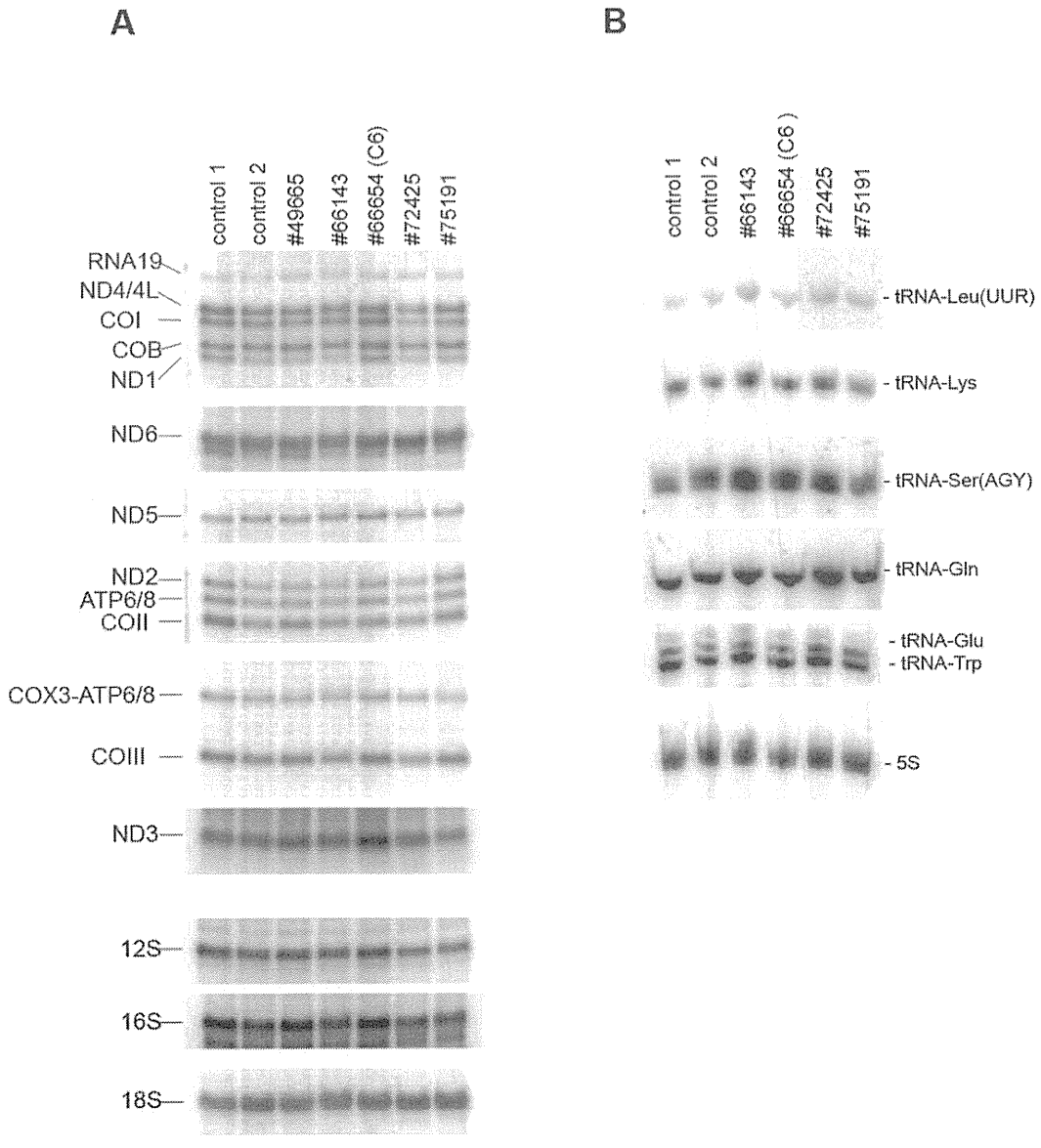

Figure S3) Northern blot analysis of the steady-state levels of mitochondrial transcripts in GTPBP3 patient fibroblasts.

A) Northern blot analysis of total RNA isolated from the *GTPBP3* patient or control primary fibroblasts. The blots were probed with the mt-mRNA- and mt-rRNA-specific probes as indicated. The cytosolic 18S rRNA was used as a loading control.

B)) High-resolution Northern blot analysis of total RNA isolated from the *GTPBP3* patient or control primary fibroblasts. The blots were probed with the mt-tRNA -specific probes as indicated. The cytosolic 5S rRNA was used as a loading control.

Figure S4

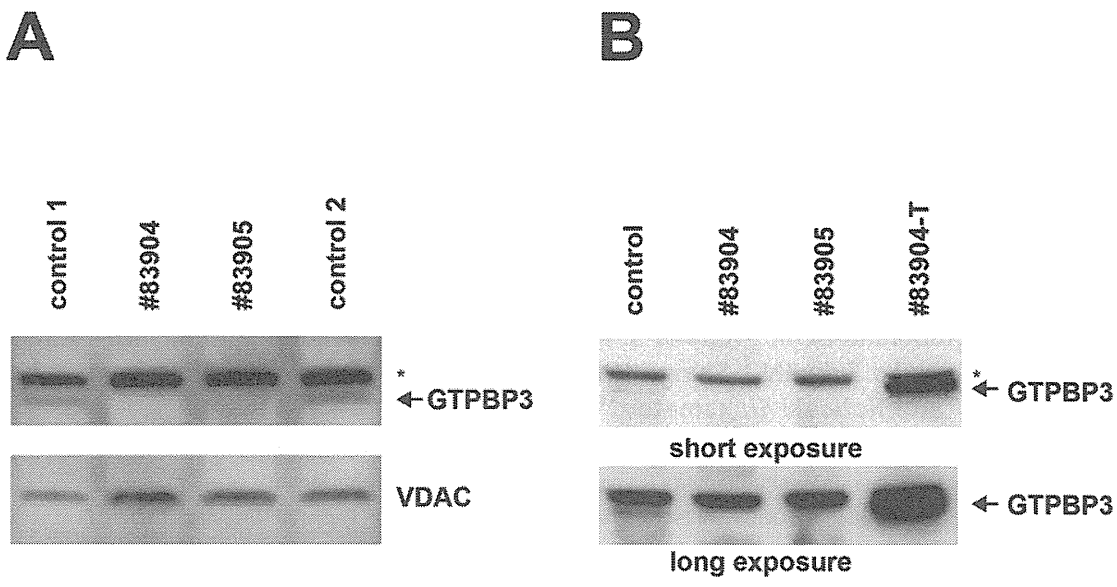

Figure S4) Analysis of GTPBP3 protein levels in patient fibroblasts

A) Immunoblot analysis of GTPBP3 protein levels in fibroblasts from affected individuals #83904 and #83905 from family F9. VDAC served as a mitochondrial loading control. (Asterics indicates a non-specific band.)

B) Comparison of the electrophoretic migration of GTPBP3 in un-transfected cells (lane control) and cells derived from one of the affected individuals transfected with a plasmid (pIRES2-EGFP) for *GTPBP3* cDNA expression (lane #83904-T). (Asterics indicates a non-specific band.)

RESEARCH ARTICLE

AMERICAN JOURNAL OF medical genetics PART A

Mutations in *HADHB*, which Encodes the β-Subunit of Mitochondrial Trifunctional Protein, Cause Infantile Onset Hypoparathyroidism and Peripheral Polyneuropathy

Misako Naiki,[1,2] Nobuhiko Ochi,[3] Yusuke S. Kato,[4] Jamiyan Purevsuren,[5] Kenichiro Yamada,[1] Reiko Kimura,[1] Daisuke Fukushi,[1] Shinya Hara,[6] Yasukazu Yamada,[1] Toshiyuki Kumagai,[7] Seiji Yamaguchi,[5] and Nobuaki Wakamatsu[1]*

[1]Department of Genetics, Institute for Developmental Research, Aichi Human Service Center, Kasugai, Aichi, Japan

[2]Department of Pediatrics, Nagoya University Graduate School of Medicine, Nagoya, Aichi, Japan

[3]Department of Pediatrics, Daini-Aoitori Gakuen, Aichi Prefectural Hospital and Habilitation Center for Disabled Children, Okazaki, Aichi, Japan

[4]Institute for Health Science, Tokushima Bunri University, Tokushima, Japan

[5]Department of Pediatrics, Shimane University, Faculty of Medicine, Izumo, Shimane, Japan

[6]Department of Pediatrics, Toyota Memorial Hospital, Toyota, Aichi, Japan

[7]Department of Pediatric Neurology, Kobato Gakuen, Aichi Human Service Center, Kasugai, Aichi, Japan

Manuscript Received: 18 July 2013; Manuscript Accepted: 16 December 2013

Mitochondrial trifunctional protein (MTP) is a hetero-octamer composed of four α- and four β-subunits that catalyzes the final three steps of mitochondrial β-oxidation of long chain fatty acids. *HADHA* and *HADHB* encode the α-subunit and the β-subunit of MTP, respectively. To date, only two cases with MTP deficiency have been reported to be associated with hypoparathyroidism and peripheral polyneuropathy. Here, we report on two siblings with autosomal recessive infantile onset hypoparathyroidism, peripheral polyneuropathy, and rhabdomyolysis. Sequence analysis of *HADHA* and *HADHB* in both siblings shows that they were homozygous for a mutation in exon 14 of *HADHB* (c.1175C>T, [p.A392V]) and the parents were heterozygous for the mutation. Biochemical analysis revealed that the patients had MTP deficiency. Structural analysis indicated that the A392V mutation identified in this study and the N389D mutation previously reported to be associated with hypoparathyroidism are both located near the active site of MTP and affect the conformation of the β-subunit. Thus, the present patients are the second and third cases of MTP deficiency associated with missense *HADHB* mutation and infantile onset hypoparathyroidism. Since MTP deficiency is a treatable disease, MTP deficiency should be considered when patients have hypoparathyroidism as the initial presenting feature in infancy.

Key words: hypoparathyroidism; MTP deficiency; HADHB; LCKT; peripheral polyneuropathy

How to Cite this Article:
Naiki M, Ochi N, Kato YS, Purevsuren J, Yamada K, Kimura R, Fukushi D, Hara S, Yamada Y, Kumagai T, Yamaguchi S, Wakamatsu N. 2014. Mutations in *HADHB*, which encodes the β-subunit of mitochondrial trifunctional protein, cause infantile onset hypoparathyroidism and peripheral polyneuropathy.
Am J Med Genet Part A 164A:1180–1187.

Conflict of Interest: The authors declare no conflict of interests.
Grant sponsor: Takeda Science Foundation; Grant sponsor: Health Labor Sciences Research Grant; Grant sponsor: Ministry of Education, Culture, Sports, Science, and Technology of Japan (to N.W.); Grant number: #21390319.

Abbreviations: MTP, mitochondrial trifunctional protein; PTH, parathyroid hormone; LCEH, long-chain enoyl-CoA hydratase; LCHAD, long-chain 3-hydroxyacyl-CoA dehydrogenase; LCKT, long-chain 3-ketoacyl-CoA thiolase; CMT, Charcot-Marie-Tooth; MCAD, medium-chain acyl-CoA dehydrogenase.

*Correspondence to:
Nobuaki Wakamatsu, M.D., Ph.D., Department of Genetics, Institute for Developmental Research, Aichi Human Service Center, 713-8 Kamiya-cho, Kasugai, Aichi 480-0392, Japan.
E-mail: nwaka@inst-hsc.jp

Article first published online in Wiley Online Library (wileyonlinelibrary.com): 24 March 2014
DOI 10.1002/ajmg.a.36434

INTRODUCTION

MTP is a hetero-octamer composed of four α- and four β-subunits and contains three different enzyme activities that catalyze the final three chain-shortening reactions in the β-oxidation of long-chain fatty acids [Uchida et al., 1992]. *HADHA* encodes the α-subunit, which has both long-chain enoyl-CoA hydratase (LCEH, EC 4.2.1.17) and long-chain 3-hydroxyacyl-CoA dehydrogenase (LCHAD, EC 1.1.1.211) activities, whereas *HADHB* encodes the β-subunit, which has only long-chain 3-ketoacyl-CoA thiolase (LCKT, EC 2.3.1.16) activity [Uchida et al., 1992]. Mutations in *HADHA* or *HADHB* cause MTP (LCEH, LCHAD, LCKT) deficiency, with decreased activity and levels of all three enzymes because of the failure of hetero-octamer formation; however, a homozygous mutation (1528G>C) in *HADHA* has been reported to cause an isolated LCHAD deficiency [IJlst et al., 1994]. MTP deficiency is characterized by a wide range of clinical features, including cardiomyopathy, hypoketonic hypoglycemia, metabolic acidosis, sudden infant death, metabolic encephalopathy, liver dysfunction, peripheral neuropathy, exercise-induced myoglobinuria, and rhabdomyolysis [Wanders et al., 1999].

Hypoparathyroidism is a rare disorder characterized by hypocalcemia and hyperphosphatemia and is caused by deficiency in parathyroid hormone (PTH) action. An epidemiological survey showed that the prevalence of idiopathic hypoparathyroidism in Japan is 1:140,000 [Nakamura et al., 2000]. Impaired secretion of PTH causes PTH-deficient hypoparathyroidism, while resistance to PTH due to a defect in the PTH receptor or insensitivity to PTH results in pseudohypoparathyroidism. Autosomal recessive forms of isolated hypoparathyroidism have been reported to be caused by mutations in *PTH*, located on chromosome 11p15 [Parkinson and Thakker, 1992] or the gene encoding the parathyroid-specific transcription factor glial cells missing B (*GCMB*) on 6p24 [Ding et al., 2001].

Here, we report that two siblings born to consanguineous parents have MTP deficiency associated with infantile onset hypoparathyroidism. We have identified a new missense mutation in *HADHB* located close to the active site of the β-subunit of MTP. We also review hypoparathyroidism caused by MTP deficiencies and discuss the pathogenesis of the disease associated with hypoparathyroidism.

PATIENTS AND METHODS

Written informed consent was obtained from the patients and the family members who participated in this study. The experiments were conducted after approval by the institutional review board at the Institute for Developmental Research, Aichi Human Service Center.

The proband (IV-1) is an 18-year-old female born to first-cousin parents as a dizygotic twin (Fig. 1A). She was born at 37 weeks and 4 days gestation by normal vaginal delivery following an uneventful pregnancy. She was hospitalized 5 weeks after birth because of generalized seizures. Biochemical analysis revealed a decreased serum calcium concentration of 1.15 mmol/L (normal range: 2.25–2.75 mmol/L) and an elevated serum phosphorus concentration of 3.49 mmol/L (normal range: 1.21–2.18 mmol/L). The serum concentration of intact-PTH (iPTH) was below detectable levels (<5 pg/ml; normal range: 10–65 pg/ml). The concentrations of serum creatinine and blood urea nitrogen (BUN) were 0.3 mg/dl (normal range: 0.1–0.4 mg/dl) and 7 mg/dl (normal range: 7–19 mg/dl), respectively; thus, renal function was normal. She was diagnosed with hypoparathyroidism and was treated with activated vitamin D and calcium. The therapy elevated the serum calcium concentration, and she no longer experienced seizures. At 1 year of age, her serum calcium concentration had increased to 2.00 mmol/L, but her serum iPTH concentration was undetectable (<5 pg/ml). She achieved all developmental milestones at the appropriate age. At 2 years, she was admitted to the hospital with tetany after an upper respiratory tract infection. Upon admission, laboratory examination revealed an elevated serum creatine kinase concentration of 9,577 U/L (normal range: 20–150 U/L) and a low serum calcium concentration of 1.48 mmol/L. She was diagnosed with rhabdomyolysis and hypocalcemia and was successfully treated with intravenous fluids. She was later admitted to the hospital with recurrent episodes of fever, hypocalcemia, rhabdomyolysis, and myoglobinuria for several years. She has also experienced distal lower limb muscle weakness and atrophy since 3 years of age. Because of having a drop foot, she has had difficulty walking and has used foot orthoses or a wheelchair since she was 9. A neurologic examination at 9 years of age demonstrated distal muscle weakness, particularly involving the peroneal muscles, with absent tendon reflexes. There were no signs of pyramidal tract involvement. The motor conduction velocity of the peroneal nerve was decreased to 21.6 m/sec (normal range: 40–65 m/sec). Sensory conduction velocity of the sural nerve could not be evoked. The Gower's sign was negative. Thus, she has peripheral sensorimotor polyneuropathy. A muscle biopsy from the left biceps brachii demonstrated denervation atrophy with a predominance of type I fibers. She currently presents with severe muscular atrophy of the lower legs and hands with an absence of Achilles and patellar tendon reflexes, which are the clinical features of Charcot-Marie-Tooth (CMT) disease. She also has a drop foot and hammer toes, and touch and vibration senses of the distal legs are diminished (Fig. 1B). The serum calcium and iPTH concentrations at present were 2.10 mmol/L and 5 pg/ml, respectively. Analysis of blood acylcarnitines and urine organic acids measured once in a non-acute phase showed no abnormalities.

Patient IV-2 is an 18-year-old male who is the dizygotic twin of Patient IV-1 (Fig. 1A). Because his twin sister had hypoparathyroidism at the age of 1 month, his serum concentration of iPTH was measured at 4 months. He was asymptomatic, but his serum iPTH concentration was undetectable (<5 pg/ml) with a decreased calcium concentration (1.50 mmol/L) and an elevated phosphorus concentration (3.97 mmol/L). He started a regimen of activated vitamin D and calcium. He did not experience seizures but developed progressive peripheral polyneuropathy, and has exhibited rhabdomyolysis triggered by fevers from viral infections since he was 3. At 9 years of age, the motor conduction velocity of the peroneal nerve was decreased to 35.6 m/sec, and sensory conduction velocity of the sural nerve was not evoked. Findings from a muscle biopsy performed at 10 years of age were similar to those obtained for his sister. At 10 years of age, he required ventilator support owing to respiratory failure following an episode of rhab-

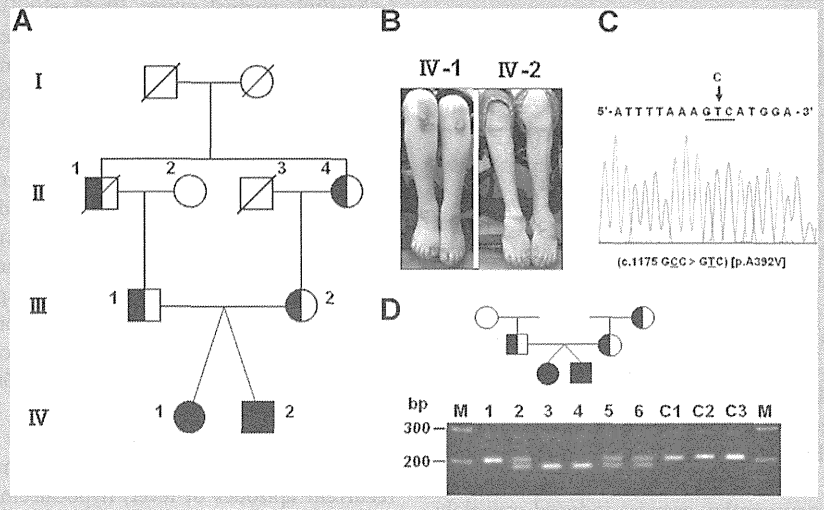

FIG. 1. The identification of the mutation in *HADHB*. A: The pedigree of the family with hypoparathyroidism and peripheral polyneuropathy. Affected individuals are indicated by filled symbols, unaffected individuals by unfilled symbols, and carrier individuals by half-filled symbols. B: The patients have muscle atrophy of the lower legs and deformity of the toes [hammer toes]. C: The direct sequence analysis of the patient IV-1 revealed a C to T substitution at nucleotide position 1175 in exon 14 of *HADHB*, resulting in the substitution of alanine [GCC] at codon 392 with valine [GTC] [c.1175C>T, [p.Ala392Val]], as indicated by the arrow. D: PCR-RFLP analysis using *Bsp*HI-digested PCR products from family members and three normal controls [C1, C2, and C3] were run through a 1.5% low-melting agarose gel. The sizes of the DNA markers are indicated on the left side.

domyolysis and myoglobinuria with a decreased calcium concentration (1.88 mmol/L) and a normal phosphorus concentration (1.93 mmol/L); however, his renal function was normal, as indicated by his serum creatinine (0.3 mg/dl) and BUN (17 mg/dl) concentrations. Analysis of blood acylcarnitines and urine organic acids in a non-acute phase showed no abnormalities. The serum calcium and iPTH concentrations at present were 2.20 mmol/L and 6 pg/ml, respectively. He currently presents with clinical features similar to those of his sister (Fig. 1B).

Patient IV-1 developed seizures due to hypoparathyroidism at 5 weeks after birth, and hypoparathyroidism was diagnosed in Patient IV-2 at the age of 4 months. Thus, both patients presented with infantile onset hypoparathyroidism. The clinical features of the presented patients are summarized in Table I.

DNA Analysis

Genomic DNA was isolated from white blood cells by phenol/chloroform extraction. Specific primers were designed to amplify *PTH*, *GCMB*, *HADHA*, and *HADHB*. PCR-amplified DNA fragments were isolated, purified, and sequenced using the Big Dye Terminator Cycle Sequencing Kit (Applied Biosystems, Foster City,

TABLE I. Clinical and Molecular Features of Hypoparathyroidism Associated With MTP Deficiency

Patients	1	2	3	4
Gender	Female	Female	Female	Male
Age at onset				
Hypoparathyroidism	15 m	4 m	5 w	4 m
Rhabdomyolysis	15 m	15 m	2 y	3 y
Peripheral polyneuropathy	15 m	4 m	3 y	3 y
Hypotonia	+	+	−	−
Liver dysfunction	+	+	−	−
HADHA/HADHB mutation	ND	N389D (HADHB)	A392V (HADHB)	A392V (HADHB)
References	Dionisi-Vici et al. [1996]	Labarthe et al. [2006]	This study	This study

+, present; −, not present; ND, not described; w, week; m, month; y, year.

CA). Mismatch primer pairs (sense: 5′-tgctgggattacagatgtgag-3′; antisense: 5′-tgcaaaccaatcagaattcatg-3′) were prepared for PCR-RFLP analysis to generate the *Bsp*HI site (tcatga) in a mutant allele. *Bsp*HI was used to digest the 200-bp mutant (c.1175C>T) PCR product, which generated the 178-bp PCR product.

Enzyme Assay

Mitochondrial LCKT activity in lymphoblastoid cells from the two patients and from two healthy adult males (as the control) was determined using 10 μM 2-ketopalmitoyl-CoA as a substrate [Purevsuren et al., 2009]. Citrate synthase activity was determined spectrophotometrically using DTNB.

MTP Expression Analysis

Cell extracts of lymphoblastoid cells from Patients IV-1 and IV-2 and two healthy adult males and of MTP-deficient fibroblasts (previously reported by Purevsuren et al. [2009]) were subjected to 12.5% sodium dodecyl sulfate-polyacrylamide gel electrophoresis (SDS-PAGE). Western blot analysis was performed using a rabbit polyclonal antibody specific for both the α- and β-subunits of MTP or medium-chain acyl-CoA dehydrogenase (MCAD) (both antibodies were generously provided by Dr. T. Hashimoto, Professor Emeritus, Shinshu University), and blots were visualized using the Immuno-Pure NBT/BCIP Substrate Kit (Promega, Madison, WI).

Construction of Wild-Type and Mutant HADHB-FLAG and Wild-Type HADHA-MYC Expression Vectors

The wild-type HADHB expression vector was prepared by subcloning *HADHB* cDNA at the *NotI*/*Eco*RV site of a mammalian expression vector, p3 × FLAG-CMV (Sigma–Aldrich, St. Louis, MO) (pHADHB-FLAG). An *Eco*RV recognition site (gatatc) was introduced at the termination codon (TAA) of *HADHB*. The mutant *HADHB* (pHADHB-A392V-FLAG, pHADHB-R61C-FLAG, pHADHB-N389D-FLAG, and pHADHB-R444K-FLAG; amino acid number is shown from the first methionine) and the wild-type *HADHA* (pHADHA-MYC) expression vectors were prepared using the in vitro mutagenesis method [Yamada et al., 2013]. The generated expression vectors encoded the FLAG-tagged wild-type or mutant β-subunits and MYC-tagged α-subunit protein at the *C*-terminus.

Analysis of the Association of the Wild-Type or Mutant β-Subunits With the Wild-Type α-Subunit

Various combinations of 0.4 μg of wild-type or mutant HADHB-FLAG expression vectors and 0.4 μg of the HADHA-MYC expression vector were co-transfected into HEK293 cells in 24-well dishes using Lipofectamine 2000 reagent (Life Technologies, Carlsbad, CA). Sixty hours after transfection, the cells were collected, and the extracts were subjected to immunoprecipitation using anti-FLAG M2 antibody-conjugated agarose (Sigma–Aldrich) for 2 hr at 4°C with gentle mixing [Yamada et al., 2013]. After washing the gels, the precipitates were subjected to a 10% SDS-PAGE, and proteins were transferred to a PVDF membrane (Immobilon-P). Western blot analysis was performed with anti-FLAG M2 antibody (for the β-subunit) and with anti-MYC antibody (for the α-subunit, kindly provided by Dr. K. Nagata, Aichi Human Service Center). Immunoreactive bands were visualized with an enhanced chemiluminescence western blotting detection system (GE Healthcare, Waukesha, WI).

Structural Analysis of MTP

A homology model of human MTP was built using the Swiss-Model automated modeling server [Kiefer et al., 2009]. N389 and A392 of the β-subunit of the MTP coordinate (PDB code: 1wdk) [Ishikawa et al., 2004] were replaced with aspartate (D) and valine (V), respectively, using the Swiss PDB Viewer [Guex and Peitsch, 1997] to determine the effect of these substitutions on the surrounding residues.

RESULTS

Identification of the Mutation

The nucleotide sequences of all exons and splice sites of the candidate genes of autosomal recessive isolated hypoparathyroidism, *PTH* and *GCMB*, revealed no mutations. Since mutations of *HADHA* and *HADHB* cause rhabdomyolysis in infancy, we determined the nucleotide sequences of all exons and intron-exon boundaries of the genes from the patients and identified a homozygous mutation (c.1175C>T, [p.A392V]) in exon 14 of *HADHB* (NM_000183) (the first methionine is numbered as one) (Fig. 1C). PCR-RFLP analysis demonstrated that the patients were homozygous, whereas the parents and grandmother were heterozygous for the mutation (Fig. 1D). The mutation was absent in 200 normal alleles.

A392V in the β-Subunit Causes MTP Deficiency

The LCKT activities of the lymphoblastoid cells of the Patients IV-1 and IV-2 were decreased to 5% and 14% of normal controls, respectively (Fig. 2A). Western blot analysis showed faint or no bands for the α- and β-subunits bands of MTP from the patient's lymphoblastoid cells. In contrast, both subunits were clearly detected in control lymphoblastoid cells (Fig. 2B). Thus, the patients were found to have MTP deficiency caused by decreased amounts of α- and β-subunits.

The A392V β-Subunit Does Not Associate With the α-Subunit of MTP

Hetero-octamer formation of the four α- and four β-subunits is necessary for MTP activity. To confirm the MTP deficiency evaluated by the enzyme assay and western blot analysis, we studied the effect of mutant β-subunits on the formation of the MTP hetero-octamer with the α-subunit by immunoprecipitation. Western blot

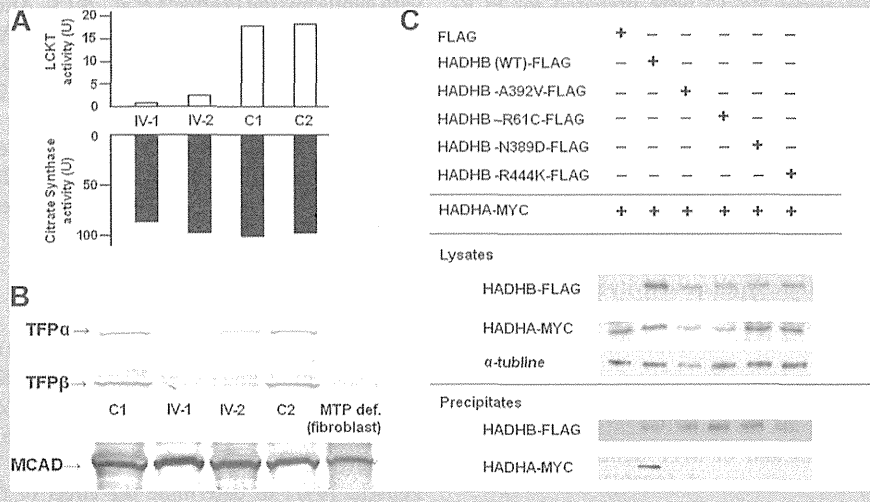

FIG. 2. Biochemical analyses of the MTP protein of the patients. A: The LCKT activities [upper panel] and citrate synthase activities [lower panel] in lymphoblastoid cells from the patients and two controls are shown [1U = μmol/min/mg protein]. B: Western blot analysis of the α- and β-subunits of MTP and MCAD protein [EC 1.3.99.3] [positive control] from the patients and controls lymphoblastoid cells and MTP-deficient fibroblasts are shown. C: Immunoprecipitation of the wild-type or mutant β-subunits with the wild-type α-subunit. [+] Indicates the FLAG- or MYC-tagged vectors used in each study. Lysates and precipitates were immunoblotted with antibodies as indicated [FLAG, MYC, and α-tubulin]. The results of western blot analysis are shown.

analysis revealed that expressions of the mutant β-subunit proteins were decreased in HEK293 cells (Fig. 2C, Lysates), but were efficiently precipitated (Fig. 2C, Precipitates). The MYC-tagged α-subunit co-precipitated with the FLAG-tagged wild-type β-subunit, whereas less than detectable levels of the α-subunit co-precipitated with the four mutant β-subunits (Fig. 2C). Thus, the A392V mutation, as well as the β-subunit N389D mutation previously reported as being associated with a hypoparathyroidism phenotype, abolished the formation of the MTP hetero-octamer, similar to other β-subunit mutations such as R61C (previously described as R28C; lethal phenotype) and R444K (previously described as R411K; neuromyopathic phenotype) [Spiekerkoetter et al., 2003; Purevsuren et al., 2009].

N389D and A392V Mutations Affect the Conformation of the β-Subunit

We analyzed a homology model of the β-subunit of human MTP. N389 and A392 of human MTP are located on the solvent-exposed surface of tetrameric MTP (Fig. 3A). These data indicated that N389 and A392 are not involved in the intersubunit interaction. The catalytic triad, composed of C138, H428, and C458 (shown as blue letters), is located very close to N389 and A392 in the homology model of human MTP (Fig. 3B). Moreover, N389 and A392 are both located on the Cα2 helix in the homology model and directly interact with the Cα1 helix. Notably, the hydrogen bond between the side chains of D389 and T356 is missing in the N389D human MTP model (Fig. 3B,C), and a slight steric clash exists between the side chains of V392 and T356 in the A392V mutant model (Fig. 3D).

DISCUSSION

MTP deficiency caused by mutations of *HADHA* or *HADHB* has been classified into three clinical phenotypes: a lethal phenotype with neonatal onset (severe form), a hepatic phenotype with infantile onset (intermediate form), and a neuromyopathic phenotype with late-adolescent onset (mild form) [Spiekerkoetter et al., 2003]. The clinical features of the patients, together with their decreased LCKT activities, the decreased protein levels of both α- and β-subunits in the patients' lymphoblastoid cells, and the failure of the mutant β-subunit to form an active hetero-octamer with the wild-type α-subunit of the MTP protein indicate that the patients presented in this study have the neuromyopathic phenotype of MTP deficiency due to a homozygous A392V mutation in *HADHB*. Spiekerkoetter et al. [2004] reported that the neuromyopathic phenotype is the major phenotype of MTP deficiency. In contrast, only two of six Japanese cases reported in the literature have presented with the neuromyopathic phenotype [Purevsuren et al., 2009; Yagi et al., 2011]. The fact that the number of cases reported with the neuromyopathic phenotype in Japan is small is most likely because this phenotype is included in the differential diagnosis of early or late-adolescent onset CMT disease with or without episodic myoglobinuria [Spiekerkoetter et al., 2004].

Only two cases of MTP deficiency associated with hypoparathyroidism have been reported (Table I). Dionisi-Vici et al. [1996] first

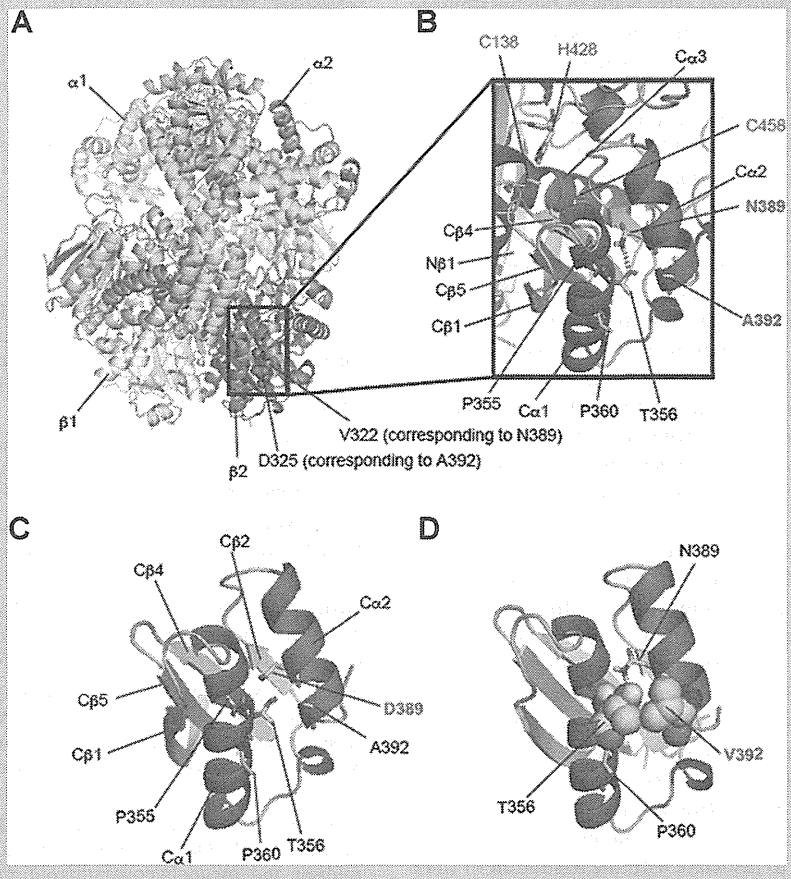

FIG. 3. Structure and homology modeling of MTP. A: α2β2 tetrameric structure of MTP. Molecules colored in cyan and green are the α-subunits [α1 and α2, respectively] of MTP from *Pseudomonas fragi*, whereas those colored in yellow and orange are the β-subunits [β1 and β2, respectively] [Ishikawa et al., 2004]. V322 and D325 are depicted as sphere models. These residues correspond to N389 and A392 of human MTP. B: Enlarged view of the homology model of one of the β-subunits of human MTP. α-helices and β-strands are colored in red and yellow, respectively. Hydrogen, carbon, oxygen, nitrogen, and sulfur atoms are colored in gray, cyan, red, blue, and yellow, respectively. Secondary structure nomenclature [Nβ1, Cβ1, Cβ4, Cβ5, Cα1, Cα2, and Cα3] defined in the yeast thiolase structure [Mathieu et al., 1997] is also indicated. Helices corresponding to Lα1 [171–175], Lα2, and Lα3 of yeast thiolase [V171-L260] have been removed for clarity. A hydrogen bond between the amino group of N389 and the hydroxyl group of T356 is depicted as a dotted line [pink]. C: View around the N389D mutation in the homology model of the β-subunit of human MTP. D: View around the A392V mutation. T356 and V392 are depicted as sphere models.

reported the case of a female patient with MTP deficiency and hypoparathyroidism. Hypoparathyroidism became apparent when she was admitted to the hospital because of fasting-induced rhabdomyolysis at 15 months of age. She had severe hypotonia, respiratory failure, and peripheral polyneuropathy without renal failure. Her serum iPTH concentration was low (4 pg/ml) with severe hypocalcemia (0.95 mmol/L), and the enzyme activities of MTP in the fibroblasts were all reduced: LCKT activity was absent, and LCHAD and LCEH activities were 30% and 52% of the control mean, respectively. These results indicate that she had MTP deficiency with a neuromyopathic phenotype, caused possibly by an *HADHB* mutation encoding LCKT. Labarthe et al. [2006] also reported a female case with hypoparathyroidism and MTP deficiency caused by a *HADHB* mutation. Hypoparathyroidism (iPTH <5 pg/ml) and severe hypocalcemia (1.2 mmol/L) became evident when she was 4 months old. A homozygous mutation (c.1165A>G, [p.N389D]) in *HADHB* was identified. Her serum iPTH concentration reached normal levels after vitamin D therapy, although she developed peripheral polyneuropathy with decreased nerve conduction velocity. LCKT activity was not reported, but numerous episodes of fasting-induced rhabdomyolysis suggested that she had a defective β-subunit of MTP. Indeed, we demonstrated that the N389D β-subunit does not associate with the wild-type α-subunit (Fig. 2C). Taken together, the sibling patients presented here and the two previously reported cases have similar clinical features of infantile onset hypoparathyroidism, peripheral polyneuropathy, and rhabdomyolysis.

A dysfunction in mitochondrial energy metabolism and/or toxicity of accumulated long-chain fatty acids in the parathyroid glands may have contributed to the pathogenesis of hypoparathyroidism in the patients with MTP deficiency [Saudubray et al., 1999]. In fact, hypoparathyroidism has also been reported in other disorders of mitochondrial fatty acid oxidation, including LCHAD deficiency [Tyni et al., 1997] and MCAD deficiency [Baruteau et al., 2009]. However, this hypothesis cannot explain why hypoparathyroidism has not been reported in patients with the most common inborn mitochondrial fatty acid β-oxidation disorders of carnitine palmitoyl transferase II and very-long-chain acyl-CoA dehydrogenase deficiencies or the severe form of MTP deficiency (a lethal phenotype). Thus, the mechanisms underlying the pathogenesis of the disease presented here remains to be elucidated. Tyni et al. [1997] reported the autopsy findings of a patient with hypoparathyroidism and LCHAD deficiency where the parathyroid glands were severely hypoplastic. These findings suggest that mutations of the proteins associated with β-oxidation cause hypoparathyroidism by congenital malformations of parathyroid glands.

Our studies demonstrate decreased expression of the mutant β-subunits (N389D and A392V) and a failure of those subunits to associate with the wild-type α-subunit (Fig. 2). Moreover, N389D and A392V are located close to the active site and are likely have an immediate impact on the structure and function of the catalytic core of human MTP (Fig. 3C,D). A recent study demonstrated that the β-subunit of MTP interacts and colocalizes with the estrogen receptor α or β in the mitochondria and suggested an important role of the β-subunit in estrogen-mediated lipid metabolism [Zhou et al., 2012a,b]. From this perspective, mutant N389D and A392V β-subunits may cause mitochondria dysfunction, including MTP deficiency due to a failure to associate with the α-subunit of MTP and other proteins that result in dysfunction of parathyroid glands. Further case studies are required to determine whether the specific mutations located in the proximity of the active site of the β-subunit are associated with hypoparathyroidism and MTP deficiency.

Early diagnosis and treatment are important for patients with the neuromyopathic phenotype of MTP deficiency, since peripheral polyneuropathy is progressive [Spiekerkoetter et al., 2004; Yamaguchi et al., 2012]. Our study has demonstrated that MTP deficiency should be considered when patients have hypoparathyroidism as the initial presenting feature in infancy.

ACKNOWLEDGMENTS

We would like to thank the patients and their family members who participated in this study. This work was supported by the Takeda Science Foundation, a Health Labor Sciences Research Grant, and a grant (#21390319) from the Ministry of Education, Culture, Sports, Science, and Technology of Japan to N.W.

REFERENCES

Baruteau J, Levade T, Redonnet-Vernhet I, Mesli S, Bloom MC, Broué P. 2009. Hypoketotic hypoglycemia with myolysis and hypoparathyroidism: An unusual association in medium chain acyl-CoA desydrogenase deficiency (MCADD). J Pediatr Endocrinol Metab 22:1175–1177.

Ding C, Buckingham B, Levine MA. 2001. Familial isolated hypoparathyroidism caused by a mutation in the gene for the transcription factor GCMB. J Clin Invest 108:1215–1220.

Dionisi-Vici C, Garavaglia B, Burlina AB, Bertini E, Saponara I, Sabetta G, Taroni F. 1996. Hypoparathyroidism in mitochondrial trifunctional protein deficiency. J Pediatr 129:159–162.

Guex N, Peitsch MC. 1997. SWISS-MODEL and the Swiss-PdbViewer: An environment for comparative protein modeling. Electrophoresis 18:2714–2723.

IJlst L, Wanders RJA, Ushikubo S, Kamijo T, Hashimoto T. 1994. Molecular basis of long-chain 3-hydroxyacyl-CoA dehydrogenase deficiency: Identification of the major disease-causing mutation in the alpha-subunit of the mitochondrial trifunctional protein. Biochim Biophys Acta 1215:347–350.

Ishikawa M, Tsuchiya D, Oyama T, Tsunaka Y, Morikawa K. 2004. Structural basis for channelling mechanism of a fatty acid beta-oxidation multienzyme complex. EMBO J 23:2745–2754.

Kiefer F, Arnold K, Künzli M, Bordoli L, Schwede T. 2009. The SWISS-MODEL Repository and associated resources. Nucleic Acids Res 37: D387–D392.

Labarthe F, Benoist JF, Brivet M, Vianey-Saban C, Despert F, de Baulny HO. 2006. Partial hypoparathyroidism associated with mitochondrial trifunctional protein deficiency. Eur J Pediatr 165:389–391.

Mathieu M, Modis Y, Zeelen JP, Engel CK, Abagyan RA, Ahlberg A, Rasmussen B, Lamzin VS, Kunau WH, Wierenga RK. 1997. The 1.8 A crystal structure of the dimeric peroxisomal 3-ketoacyl-CoA thiolase of *Saccharomyces cerevisiae*: Implications for substrate binding and reaction mechanism. J Mol Biol 273:714–728.

Nakamura Y, Matsumoto T, Tamakoshi A, Kawamura T, Seino Y, Kasuga M, Yanagawa H, Ohno Y. 2000. Prevalence of idiopathic hypoparathyroidism and pseudohypoparathyroidism in Japan. J Epidemiol 10: 29–33.

Parkinson DB, Thakker RV. 1992. A donor splice site mutation in the parathyroid hormone gene is associated with autosomal recessive hypoparathyroidism. Nat Genet 1:149–152.

Purevsuren J, Fukao T, Hasegawa Y, Kobayashi H, Li H, Mushimoto Y, Fukuda S, Yamaguchi S. 2009. Clinical and molecular aspects of Japanese patients with mitochondrial trifunctional protein deficiency. Mol Genet Metab 98:372–377.

Saudubray JM, Martin D, de Lonlay P, Touati G, Poggi-Travert F, Bonnet D, Jouvet P, Boutron M, Slama A, Vianey-Saban C, Bonnefont JP, Rabier D, Kamoun P, Brivet M. 1999. Recognition and management of fatty acid oxidation defects: A series of 107 patients. J Inherit Metab Dis 22: 488–502.

Spiekerkoetter U, Sun B, Khuchua Z, Bennett MJ, Strauss AW. 2003. Molecular and phenotypic heterogeneity in mitochondrial trifunctional protein deficiency due to beta-subunit mutations. Hum Mutat 21: 598–607.

Spiekerkoetter U, Bennett MJ, Ben-Zeev B, Strauss AW, Tein I. 2004. Peripheral neuropathy, episodic myoglobinuria, and respiratory failure in deficiency of the mitochondrial trifunctional protein. Muscle Nerve 29:66–72.

Tyni T, Rapola J, Palotie A, Pihko H. 1997. Hypoparathyroidism in a patient with long-chain 3-hydroxyacyl-coenzyme A dehydrogenase deficiency caused by the G1528C mutation. J Pediatr 131:766–768.

Uchida Y, Izai K, Orii T, Hashimoto T. 1992. Novel fatty acid beta-oxidation enzymes in rat liver mitochondria. II. Purification and prop-

erties of enoyl-coenzyme A (CoA) hydratase/3-hydroxyacyl-CoA dehydrogenase/3-ketoacyl-CoA thiolase trifunctional protein. J Biol Chem 267:1034–1041.

Wanders RJ, Vreken P, den Boer ME, Wijburg FA, van Gennip AH, IJlst L. 1999. Disorders of mitochondrial fatty acyl-CoA beta-oxidation. J Inherit Metab Dis 22:442–487.

Yagi M, Lee T, Awano H, Tsuji M, Tajima G, Kobayashi H, Hasegawa Y, Yamaguchi S, Takeshima Y, Matsuo M. 2011. A patient with mitochondrial trifunctional protein deficiency due to the mutations in the HADHB gene showed recurrent myalgia since early childhood and was diagnosed in adolescence. Mol Genet Metab 104:556–559.

Yamada K, Takado Y, Kato YS, Yamada Y, Ishiguro H, Wakamatsu N. 2013. Characterization of the mutant β-subunit of β-hexosaminidase for dimer formation responsible for the adult form of Sandhoff disease with the motor neuron disease phenotype. J Biochem 153:111–119.

Yamaguchi S, Li H, Purevsuren J, Yamada K, Furui M, Takahashi T, Mushimoto Y, Kobayashi H, Hasegawa Y, Taketani T, Fukao T, Fukuda S. 2012. Bezafibrate can be a new treatment option for mitochondrial fatty acid oxidation disorders: Evaluation by in vitro probe acylcarnitine assay. Mol Genet Metab 107:87–91.

Zhou Z, Zhou J, Du Y. 2012a. Estrogen receptor beta interacts and colocalizes with HADHB in mitochondria. Biochem Biophys Res Commun 427:305–308.

Zhou Z, Zhou J, Du Y. 2012b. Estrogen receptor alpha interacts with mitochondrial protein HADHB and affects beta-oxidation activity. Mol Cell Proteomics 11:M111.011056.

ANNALS of Clinical and Translational Neurology
Open Access
ANA American Neurological Association

RESEARCH PAPER

New *MT-ND6* and *NDUFA1* mutations in mitochondrial respiratory chain disorders

Natsumi Uehara[1,2], Masato Mori[3], Yoshimi Tokuzawa[1], Yosuke Mizuno[1], Shunsuke Tamaru[1], Masakazu Kohda[1,4], Yohsuke Moriyama[1], Yutaka Nakachi[1,4], Nana Matoba[4], Tetsuro Sakai[5], Taro Yamazaki[5], Hiroko Harashima[5], Kei Murayama[6], Keisuke Hattori[7], Jun-Ichi Hayashi[7], Takanori Yamagata[3], Yasunori Fujita[8], Masafumi Ito[8], Masashi Tanaka[9], Ken-ichi Nibu[2], Akira Ohtake[5] & Yasushi Okazaki[1,4]

[1]Division of Functional Genomics & Systems Medicine, Research Center for Genomic Medicine, Saitama Medical University, Hidaka, Japan
[2]Department of Otolaryngology-Head and Neck Surgery, Kobe University Graduate School of Medicine, Kobe, Japan
[3]Department of Pediatrics, Jichi Medical University, Shimotsuke, Japan
[4]Division of Translational Research, Research Center for Genomic Medicine, Saitama Medical University, Hidaka, Japan
[5]Department of Pediatrics, Faculty of Medicine, Saitama Medical University, Moroyama-machi, Japan
[6]Department of Metabolism, Chiba Children's Hospital, Chiba, Japan
[7]Faculty of Life and Environmental Sciences, University of Tsukuba, Tsukuba, Japan
[8]Research Team for Mechanism of Aging, Tokyo Metropolitan Institute of Gerontology, Itabashi, Japan
[9]Department of Genomics for Longevity and Health, Tokyo Metropolitan Institute of Gerontology, Itabashi, Japan

Correspondence
Yasushi Okazaki, Division of Functional Genomics & Systems Medicine, Research Center for Genomic Medicine, Saitama Medical University, 1397-1 Yamane, Hidaka, Saitama 350-1241, Japan. Tel: +81-42-984-0448; Fax: +81-42-984-0449; E-mail: okazaki@saitama-med.ac.jp
Akira Ohtake, Department of Pediatrics, Faculty of Medicine, Saitama Medical University, 38 Morohongo, Moroyama-machi, Iruma-gun, Saitama 350-0495, Japan. Tel: +81-49-276-1220; Fax: +81-49-276-1790; E-mail: akira_oh@saitama-med.ac.jp

Funding Information
This study was supported in part by a grant from the Research Program of Innovative Cell Biology by Innovative Technology (Cell Innovation), a Grant-in-Aid for the Development of New Technology from The Promotion and Mutual Aid Corporation for Private Schools of Japan from MEXT (to Y. O.), a Grant-in-Aid research grants for Scientific Research (A-22240072, B-21390459, A-25242062) from the Ministry of Education, Culture, Sports, Science, and Technology (MEXT) of Japan to M. T., and a Grant-in-Aids (H23-016, H23-119, and H24-005) for the Research on Intractable Diseases (Mitochondrial Disease) from the Ministry of Health, Labour and Welfare (MHLW) of Japan to M. T. and A. O., and a Grant-in-Aids (H23-001, H24-017, H24-071) for the Research on Intractable Diseases from the Ministry of Health, Labour and Welfare (MHLW) of Japan to A. O.

Abstract

Objective: Mitochondrial respiratory chain disorder (MRCD) is an intractable disease of infants with variable clinical symptoms. Our goal was to identify the causative mutations in MRCD patients. **Methods**: The subjects were 90 children diagnosed with MRCD by enzyme assay. We analyzed whole mitochondrial DNA (mtDNA) sequences. A cybrid study was performed in two patients. Whole exome sequencing was performed for one of these two patients whose mtDNA variant was confirmed as non-pathogenic. **Results**: Whole mtDNA sequences identified 29 mtDNA variants in 29 patients (13 were previously reported, the other 13 variants and three deletions were novel). The remaining 61 patients had no pathogenic mutations in their mtDNA. Of the 13 patients harboring unreported mtDNA variants, we excluded seven variants by manual curation. Of the remaining six variants, we selected two Leigh syndrome patients whose mitochondrial enzyme activity was decreased in their fibroblasts and performed a cybrid study. We confirmed that m.14439G>A (*MT-ND6*) was pathogenic, while m.1356A>G (*mitochondrial 12S rRNA*) was shown to be a non-pathogenic polymorphism. Exome sequencing and a complementation study of the latter patient identified a novel c.55C>T hemizygous missense mutation in the nuclear-encoded gene *NDUFA1*. **Interpretation**: Our results demonstrate that it is important to perform whole mtDNA sequencing rather than only typing reported mutations. Cybrid assays are also useful to diagnose the pathogenicity of mtDNA variants, and whole exome sequencing is a powerful tool to diagnose nuclear gene mutations as molecular diagnosis can provide a lead to appropriate genetic counseling.

Received: 11 December 2013; Revised: 11 February 2014; Accepted: 18 March 2014

***Annals of Clinical and Translational Neurology* 2014; 1(5): 361–369**

doi: 10.1002/acn3.59

Introduction

The mitochondrial respiratory chain (RC) is a pathway for vital energy generation in which ATP is generated as a form of energy by the substrates generated from glycolysis and β-oxidation. The pathway is composed of five multi-enzyme complexes (complexes I–V), two electron carriers, a quinone (coenzyme Q), and a small hem-containing protein (cytochrome c) that are located in the inner mitochondrial membrane. These RC complexes are formed from subunits encoded by both mitochondrial DNA (mtDNA) and nuclear DNA (nDNA), with the exception of complex II, which is entirely encoded by nDNA.

mtDNA is a circular double-stranded DNA molecule ~16 kb in length that encodes 37 genes comprising 13 proteins, 22 mitochondrial tRNAs, and 2 rRNAs.[1,2] Defects in mitochondrial function are associated with numerous neurodegenerative diseases, such as Parkinson's disease, Alzheimer's disease, and Huntington's disease, and, in particular with mitochondrial respiratory chain disorder (MRCD). MRCD is genetically, clinically, and biochemically heterogeneous, and it can give rise to any symptoms, in any organs or tissues, at any age and with any mode of inheritance.[3] One in 5000 births is a conservative realistic estimate for the minimum birth prevalence of MRCD.[4] Especially in children, MRCD is an intractable disease and can be regarded as the most common group of inborn errors of metabolism.[5,6]

Some MRCD patients have typical clinical findings that are caused by specific point mutations or large deletions of mtDNA. Typical clinical features include mitochondrial myopathy, encephalopathy, lactic acidosis, and stroke-like episodes (MELAS), myoclonus epilepsy associated with ragged-red fibers (MERRF), Leber's hereditary optic neuropathy (LHON), and chronic progressive external ophthalmoplegia (CPEO).[2] Although mtDNA mutations or deletions are usually found in adults showing typical clinical findings, they account for only a minority of children with MRCD. Therefore, the diagnosis of MRCD in children by screening known mtDNA mutations is rather difficult.[7] Hence, a combination of general biochemical study, histological study, and genetic analysis is essential for the diagnosis of MRCD, especially in children.[6]

In this study, we performed whole mtDNA sequencing for 90 children diagnosed with MRCD by RC enzyme assay with the aim of identifying causative mtDNA mutations.

Subjects, Materials, and Methods

Patients

Ninety Japanese pediatric patients diagnosed with MRCD and without characteristic clinical syndromes were studied. The primary diagnosis for these patients was definite or probable MRCD based on the criteria of Bernier et al.,[8] and a mitochondrial RC residual enzyme activity of <20% in a tissue, <30% in a fibroblast cell line, or <30% in two or more tissues (Data S1). Informed consent was obtained from the patients and their families before participation in the study.

Patient summaries are shown in Tables 1, 2. The details of the two patients studied in the cybrid assay are as follows: Patient (Pt) 377 is a 1-year-old girl born after a normal pregnancy to non-consanguineous parents. She has a normal brother and sister. She was hospitalized with gait difficulties at the age of 1 year. Blood lactate levels were high. Brain magnetic resonance imaging (MRI)

Table 1. Distribution of mtDNA variants and clinical features.

Characteristics		Non-pathogenic mutations	Low probability variants	New pathogenic deletions	Known variants	Total
Number of subjects		61 (100%)	13 (100%)	3 (100%)	13 (100%)	90 (100%)
No consanguinity		57 (93%)	12 (92%)	3 (100%)	11 (85%)	84 (93%)
Age at onset	≤1 y.o.	54 (89%)	10 (77%)	3 (100%)	9 (69%)	76 (84%)
Status	Alive	33 (54%)	7 (54%)	1 (33%)	11 (85%)	53 (59%)
	Dead	28 (46%)	6 (46%)	2 (67%)	2 (15%)	37 (41%)
Sex	Female	30 (49%)	3 (23%)	2 (67%)	6 (46%)	41 (46%)
	Male	31 (51%)	10 (77%)	1 (33%)	7 (54%)	49 (54%)

y.o., years old.

Table 2. Summary of unreported mutations and deletions.

Patient ID	Age at onset	Clinical diagnosis	Enzyme assay (organ)	mtDNA variation	Locus	Heteroplasmy
377	1 year	LD	1 (Fb)	m.14439G>A	*ND6*	Homo (Fb)
190	1 year 6 months	LD	1,4 (M)	m.11246G>A	*ND4*	73% (fb)
508	0 days	SIDS	1 (Hep,Car)	m.4638A>G	*ND2*	86% (Fb), 0% (Hep, Car)
004	0 months	MC	1 (Fb)	m.5537A>G[1]	*tRNATrp*	27.4% (Fb)
271	0 months	ELBW	1 (Hep)	m.10045T>C	*tRNAGly*	Homo (hep)
312[2]	5 years	LD	1 (Fb) probably	m.1356A>G	*12S rRNA*	66% (Fb)
372	2 days	LIMD	1 (Hep)	Deletion (3424 bp) nt12493-15916		65.7% (Fb), 89.9% (Hep)
336	11 months	HD	1 (Hep)	Deletion (6639 bp) nt7734-14372		9.2% (Fb), 92.6% (Hep)
390	0 days	MC	1,4 (M,Hep)	Deletion (5424 bp) nt8574-13997		44.9% (Fb), 86.4% (Hep)

LIMD, lethal infantile mitochondrial disorder; HD, hepatic disease; LD, Leigh's disease; MC, mitochondrial cytopathy; SIDS, sudden infant death syndrome; ELBW, extremely low birth weight infant; Fb, fibroblast; Hep, liver; Car, heart; M, muscle.
[1]Expected to be causative because of the other reported mutation on the same position.
[2]m.1356A>G was confirmed as non-pathogenic and nDNA mutation was identified in Pt312.

showed bilateral and symmetrical hyperintensity foci in the basal ganglia. She developed progressive motor regression and became bedridden. Pt312 is a 5-year-old boy born after 36 weeks' gestation following a normal pregnancy to non-consanguineous parents. His birth weight was 2154 g. He has a sister who is his fraternal twin. At 5 months of age, his parents noticed hypotonia and nystagmus. At 10 months of age, he had generalized epilepsy and blood lactate and his pyruvate levels were high. A brain MRI revealed symmetrical high T2 signals in the midbrain.

Whole mtDNA sequencing and detection of variants

Genomic DNA (gDNA) was extracted from skin fibroblasts (Data S1), blood, liver, and cardiac muscle using either phenol/chloroform- or column-based extraction. Whole mtDNA was first polymerase chain reaction (PCR)-amplified as two separate large amplicons (LA1 and LA2) avoiding the nonspecific amplifications from nDNA.[9] Second-round PCR was performed using 46 primer pairs (mitoSEQrTM; Applied Biosystems, Carlsbad, CA) and the LA1 and LA2 amplicon mixture from first-round PCR as a template. PCR conditions were as follows: first-round PCR was performed in a reaction mixture containing 0.2 mmol/L of each dNTP, 0.25 U of Takara Ex Taq (Takara Bio, Shiga, Japan), 1× Ex Taq Buffer, 0.3 μmol/L of each primer, and extracted gDNA in a total volume of 50 μL. Initial denaturation was performed at 94°C for 2 min, followed by 30 cycles of 94°C for 20 sec, 60°C for 20 sec, and 72°C for 5 min, with a final extension at 72°C for 11 min. Second-round PCR was performed in a reaction mixture as above except with a 10,000-fold dilution of LA1 amplicon and a 100-fold dilution of LA2 amplicon (total volume of the PCR reaction, 10 μL). Initial denaturation was performed at 96°C for 5 min, followed by 30 cycles of 94°C for 30 sec, 60°C for 45 sec, and 72°C for 45 sec, with a final extension at 72°C for 10 min.

First- and second-round PCR products were separated by 1% and 2% agarose gels, respectively, then 10 μL of second-round PCR products were incubated with 1 μL of ExoSAP-IT reagent (GE Healthcare UK Ltd., Bucks, U.K.) at 37°C for 30 min to degrade remaining primers and nucleotides. The ExoSAP-IT reagent was then inactivated by incubating at 75°C for 15 min. PCR products were sequenced using a BigDye Terminator v3.1 cycle sequencing kit (Applied Biosystems) and an ABI3130xl Genetic Analyzer (Applied Biosystems). Sequence data were compared with the revised Cambridge sequence (GenBank Accession No. NC_012920.1) and sequences present in MITOMAP (http://mitomap.org/MITOMAP) and mtSNP (http://mtsnp.tmig.or.jp/mtsnp/index_e.shtml) using SeqScape software (Applied Biosystems). Whole mtDNA sequencing of seven samples was obtained using an Ion PGM™ sequencer (Life Technologies Corporation, Carlsbad, CA).

Characterization of mtDNA deletions

We searched for mtDNA deletions by focusing on the size of first-round PCR products in agarose electrophoresis. If PCR products were smaller than controls, we suspected mtDNA deletion and performed further analysis. The smaller PCR products were recovered from the gel and amplified by second-round PCR, as described above, and

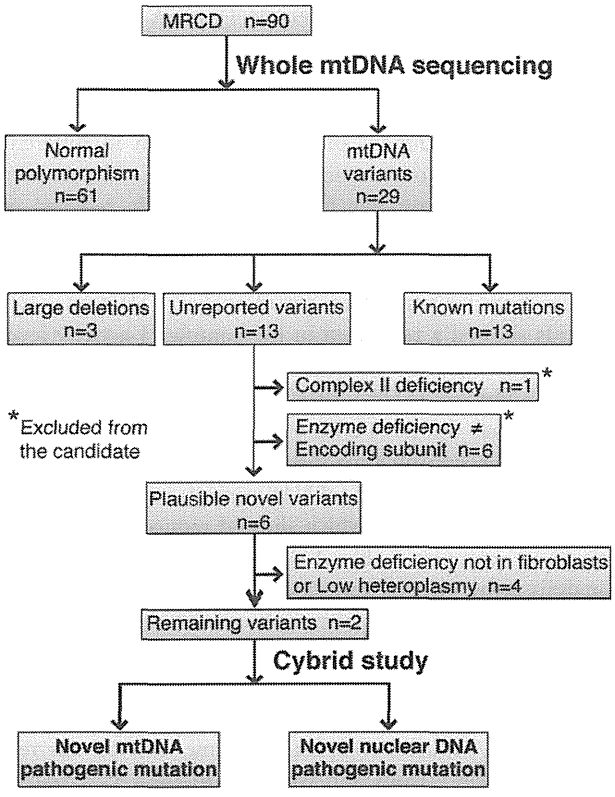

Figure 1. Flow diagram of study analysis. Ninety MRCD patients were analyzed in this study. Sixty-one patients had normal polymorphisms and 29 had mtDNA variants. Of these variants, 13 patients had MRCD causative mutations that had been previously described. We identified three novel large deletions and 13 unreported variants. Of the unreported variants, one patient with complex II deficiency was excluded because complex II is not encoded by mtDNA. Six patients were excluded because their enzyme deficiency pattern did not coincide with the variants found in mtDNA. Four patients were excluded because of the lack of fibroblast enzyme deficiency or low heteroplasmy. The remaining two cases were analyzed by cybrid study.

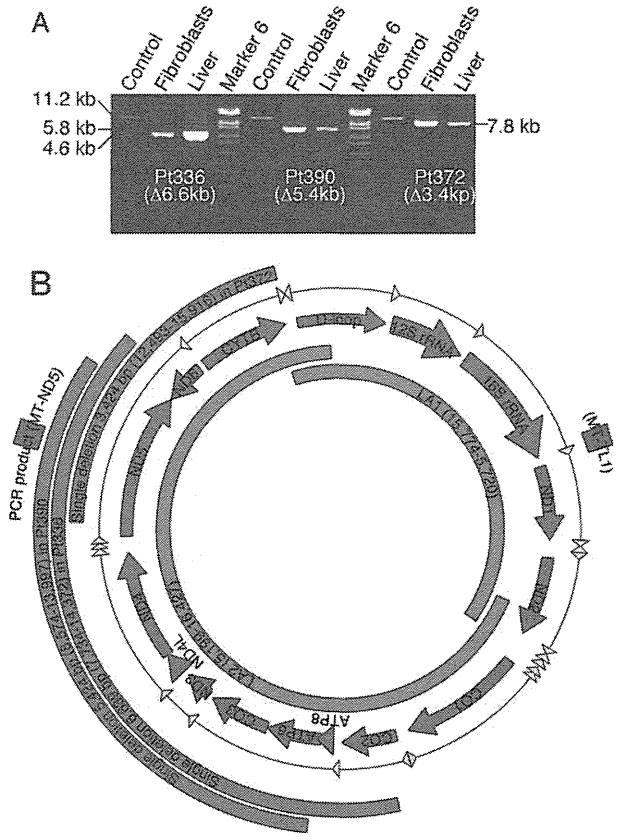

Figure 2. Identification of three large deletions. (A) Characterization of the three novel mtDNA deletions using agarose electrophoresis. First-round PCR products amplified from patient fibroblast and liver DNA clearly showed the presence of mtDNA deletions in Pt336, 390, and 372. Normal mtDNA from an MRCD patient was used as a positive control. (B) Positions of the novel mtDNA deletions are shown in blue. LA1 and LA2 amplification is shown in green. Two red squares represent real-time PCR amplicons MT-ND5 and MT-TL1.

analyzed for an mtDNA deletion. Second-round PCR was performed using fewer (25–26) PCR cycles to avoid untargeted DNA amplification. To identify the location of the deletion, we first compared the density of bands and screened the faint bands with agarose electrophoresis. The precise deletion boundaries were confirmed by sequencing analysis with primers used for second-round PCR that were close to the probable deletion region.

Results

Patient characteristics and their mtDNA mutations

A total of 90 patients (49 were men and 41 were women) with MRCD were subjected to whole mtDNA sequencing analysis (Table 1). Eighty-four subjects (93%) were non-consanguineous. Seventy-six subjects (84%) were aged 1 year or younger. We identified 13 previously reported mtDNA mutations, 13 unreported variants, and three novel deletions (Fig. 1). The remaining 61 subjects had normal polymorphisms in their mtDNA (Fig. 1).

Large mtDNA deletions were identified in three patients

Agarose gel electrophoresis of first-round PCR from fibroblast and liver mtDNA clearly showed the presence of mtDNA deletions in Pt336, 390, and 372 (Fig. 2A). The precise deletion sites were confirmed by sequencing analysis. The expected size of the first-round PCR LA2 product in wild-type mtDNA from an MRCD patient was 11.2 kb, which enabled us to estimate the deletion sizes

of Pt336, 390, and 372 as 6639, 5424, and 3424 bp, respectively (Fig. 2A and B). In Pt336, the 6639-bp deletion was located between nucleotides 7734 and 14,372 and was flanked by 5-bp perfect direct repeats. This deletion results in the loss of 15 genes (*CO2, ATP8, ATP6, CO3, ND3, ND4L, ND4, ND5, ND6*, and six *tRNA* genes). The heteroplasmy ratio of this deletion was 9.2% in the fibroblasts (Fb) and 92.6% in the liver (Hep) (Table 2 and Data S1). In Pt390, the 5424-bp deletion was located between nucleotide positions 8574 and 13,997 and was flanked by 11-bp imperfect direct repeats. This deletion results in the loss of 11 genes (*ATP6, CO3, ND3, ND4L, ND4, ND5*, and five *tRNA* genes). The heteroplasmy ratio of this deletion was 44.9% (Fb) and 86.4% (Hep) (Table 2). In Pt372, the 3424-bp deletion was located between nucleotides 12,493 and 15,916 and was flanked by 6-bp imperfect direct repeats. This deletion results in the loss of five genes (*ND5, ND6, CYB*, and two *tRNA* genes). The heteroplasmy ratio of this deletion was 65.7% (Fb), and 89.9% (Hep) (Table 2).

Unreported variants of mtDNA detected in 13 patients

We identified 13 unreported mtDNA variants. Of these, seven were excluded by manual curation (Fig. 1). One of these was excluded because the enzyme deficiency was specific to complex II, which is not encoded by mtDNA. The other six were excluded because their enzyme deficiency pattern did not coincide with the variants found in mtDNA. From the remaining six plausible mtDNA variants, we determined whether they were causative using the following inclusion criteria for further analysis: (1) cells were viable for further assay, (2) mtDNA variants corresponded to the enzyme assay data in the RC subunit, (3) enzyme deficiency was observed in the fibroblasts, and (4) variants had high heteroplasmy ratios (Fig. 1 and Table 2). On the basis of these criteria, we selected two patients whose mtDNA variants (m.14439G>A in *MT-ND6* and m.1356A>G in *12S rRNA*) were suitable for further analysis as shown in Figure 1. The other four patients were excluded because they did not show enzyme deficiency in their fibroblasts or because of low heteroplasmy ratios (Table 2).

m.14439G>A (*MT-ND6*), but not m.1356A>G (12S rRNA), is a causative mutation

The m.14439G>A (*MT-ND6*) variant was observed in fibroblasts from Pt377 (Fig. 3A). PCR- restriction fragment length polymorphism (RFLP) analysis with the *Hpy*188I restriction enzyme found Pt377 fibroblasts to be homoplasmic, and the m.14439G>A variant was not detected in the blood of the patient's parents (Fig. 3A and B). This mutation changes the proline to a serine at amino acid position 79, which is highly conserved among vertebrates (Fig. 3C). ND6 is one of the mtDNA-encoded complex I subunits and alignment of the ND6 protein in different species revealed conservation of amino acids. The activity level of the RC complex I was coincidentally reduced in the patient's fibroblasts (Fig. 4A). To further confirm whether this mutation was causative of mitochondrial dysfunction, we performed cybrid analysis (Data S1). The cybrids showed a reduction in the complex I activity level consistent with the respiratory enzyme assay in the patient's fibroblasts (Fig. 4B). These data strongly support the idea that the m.14439G>A (*ND6*) mutation detected in Pt377 is responsible for the complex I deficiency.

The m.1356A>G (*12S rRNA*) variant was observed in fibroblasts from Pt312, which showed reduced activity levels of RC complex I (Fig. 4A). By mismatch PCR-RFLP-analysis using the *Sty*I restriction enzyme, this variant was determined at a heteroplasmy ratio of 66% in the patient's fibroblasts (Table 2). The cybrids harboring this variant showed a recovery of complex I enzyme activity compared with the original patient's fibroblasts (Fig. 4B). These data suggest that reduced complex I enzyme activity was rescued by nuclear DNA and that this mtDNA variation is not causative. This further indicates that the nuclear gene mutation is the cause of MRCD in this patient.

Identification of the c.55C>T (*NDUFA1*) mutation in Pt312 by whole exome sequencing

To search for the causative nuclear gene mutation in Pt312, we performed whole exome sequencing (Data S1). This identified a single hemizygous mutation (c.55C>T) in exon 1 of the *NDUFA1* gene, which altered the amino acid residue at position 19 from proline to serine (p. P19S). The mutation was confirmed by Sanger sequencing (Fig. 5A). This conserved proline residue lies within the hydrophobic N-terminal side constituting a functional domain that is involved in mitochondrial targeting, import, and orientation of *NDUFA1*.[10,11] SIFT and PolyPhen, which predict the function of non-synonymous variants (http://genetics.bwh.harvard.edu/pph/), also revealed that the p.P19S mutation "probably" damages the function of the NDUFA1 protein (damaging score, 0.956). Alignment of the NDUFA1 protein between different species revealed the conservation of three amino acids, including the proline at position 19, which is highly conserved among vertebrates (Fig. 5B). To further confirm if the complex I deficiency in Pt312 occurred because of the mutation in *NDUFA1*, we overexpressed *NDUFA1* cDNA to determine if the enzyme deficiency

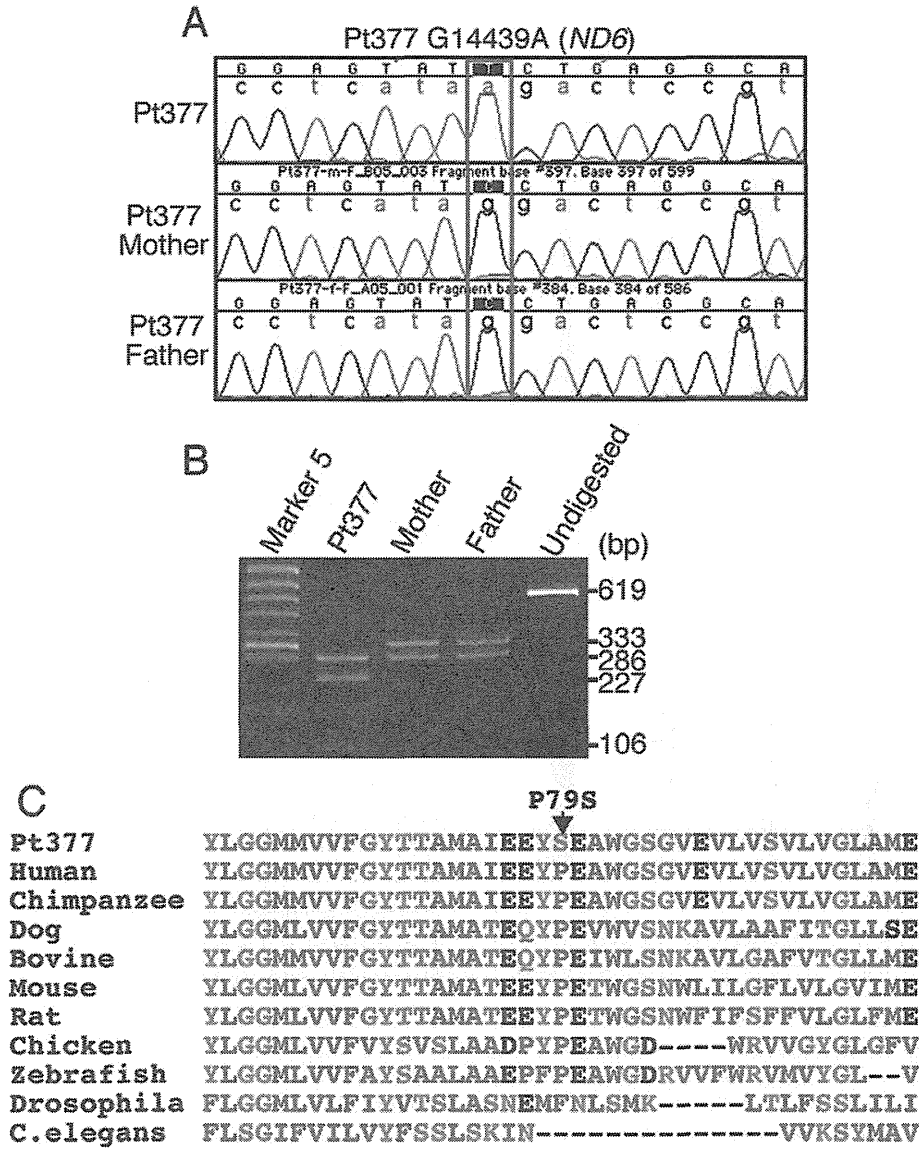

Figure 3. Novel mutation m.14439G>A in Pt377 mtDNA. (A) Trio-sequencing analysis of m.14439G>A (*MT-ND6* p.P79S) change in Pt377 family. Sequence chromatograms show that the m.14439G>A is detectable only in Pt377. (B) PCR-RFLPanalysis using fibroblast mtDNA from Pt377 and blood from both parents. A 619-bp PCR fragment was digested with *Hpy*188I. Wild-type mtDNA was cleaved into two fragments of 333 and 286 bp as shown in "Mother" and "Father", whereas the PCR product containing the m.14439G>A mutation was cleaved into three fragments: 286, 227, and 106 bp ("Pt377"). Undigested = undigested PCR product. (C) Alignment of MT-ND6 protein between different species shows the conservation of amino acid Proline 79. Amino acid sequences of *MT-ND6* gene products were aligned by ClustalW program (http://www.ebi.ac.uk/Tools/msa/clustalw2/) and NCBI/homologene (http://www.ncbi.nlm.nih.gov/homologene).

could be recovered (Data S1). Lentiviral transfection of NDUFA1 resulted in a significant increase in complex I assembly level as determined by blue native polyacrylamide gel electrophoresis. By contrast, lentiviral transfection of control mtTurboRFP did not rescue the phenotype (Fig. 5C). These data indicate that the c.55C>T mutation in *NDUFA1* is responsible for the complex I deficiency in Pt312.

Discussion

MRCD is particularly difficult to diagnose in pediatric cases as the clinical features are highly variable. We, therefore, propose a systematic approach for diagnosing MRCD that starts with a biochemical enzyme assay and is followed by whole mtDNA sequencing. In this study, we performed whole mtDNA sequencing for 90 children with

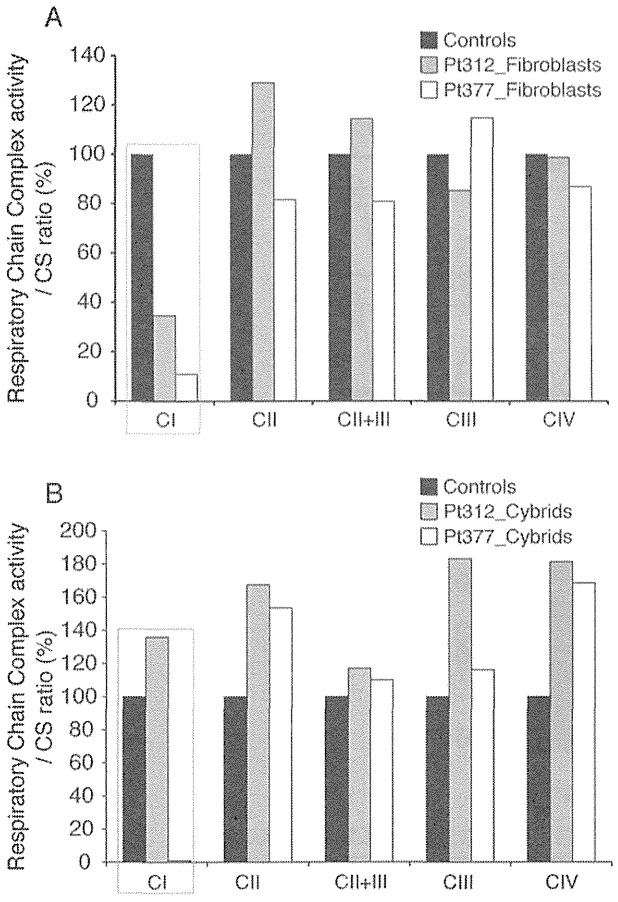

Figure 4. Biochemical assay for respiratory chain enzyme activity in fibroblasts and cybrid cells from Pt377 and Pt312. (A) Respiratory chain complex enzyme activity for *CI*, *CII*, *CII + III*, and *CIV* in skin fibroblast mitochondria from Pt312 and Pt377 compared with normal controls. The activity of each complex was calculated as a ratio relative to citrate synthase (CS). CI showed a reduction in enzyme activity in Pt312 and 377 fibroblasts. (B) Respiratory chain complex enzyme activity of cybrids established from Pt312 and Pt377 fibroblasts. Cybrids were established from rho0-HeLa cell and Pt312 or Pt377 fibroblasts. The activity of each complex in these cybrids was calculated as a ratio relative to that of citrate synthase (CS).

MRCD, and identified 29 mtDNA variants. Of these, we identified 13 known causative mutations, three large deletions, and further confirmed that m.14439G>A (*MT-ND6*) and c.55C>T (*NDUFA1*) are new causative mutations for MRCD from the results of a cybrid assay, whole exome sequencing, and a complementation study. The diagnosis of MRCD was then confirmed as definite by molecular analysis in these 18 cases.

Whole mitochondrial DNA sequencing identified 13 cases (14%) harboring known causative mtDNA mutations. mt. 10191T>C (*ND3*) and mt. 8993T>C or G (*ATP6*) mutations were detected in three and two patients, respectively (data not shown). Both are common causative mutations of infantile Leigh syndrome. Previous reports found that most common MRCD causative mutations are primarily responsible for adult-onset disease, whereas few are responsible for childhood-onset MRCD;[12,13] only 14% of our cases were attributed to known mtDNA mutations.

Most patients in this study were 1-year old or younger at the onset of disease, with no family history. We used the RC complex enzyme assay to diagnose pediatric patients who had not been diagnosed with MRCD in a clinical setting. Several MRCD cases in children were previously reported to be difficult to diagnose with nonspecific clinical presentations in contrast to the characteristic clinical syndromes such as MELAS and MERRF caused by common mtDNA mutations.[6,12]

We identified three novel deletions that we concluded were causative because they include several genes that could explain the deficiency of the RC enzymes. Generally, most mtDNA deletions share similar structural characteristics, are located in the major arc between two proposed origins of replication (OH and OL; Mitomap), and are predominantly (~85%) flanked by short direct repeats.[14,15] Single mtDNA deletions are reported to be the common causes of sporadic MRCD such as Kearns-Sayre syndrome (KSS), CPEO, and Pearson's syndrome. In this study, all three deletions were located in the major arc and were flanked by repeat sequences, similar to previous studies. Although Pt390 was diagnosed with Pearson's syndrome, the other two patients (Pt336 and Pt372) did not show a common phenotype caused by a single deletion such as KSS, CPEO, or Pearson's syndrome. Therefore, screening by mtDNA size differences is important even in those patients not clinically suspected to have mtDNA deletions.

Manual curation identified six plausible mtDNA variants that had not previously been reported (Fig. 1). We attempted to carry out a functional assay of the two patients whose fibroblasts are enzyme deficient, although it was difficult to apply this strategy to those fibroblasts with normal enzyme activity. In this sense, it is important to collect patients with similar phenotypes and carrying the same mtDNA variants to accurately diagnose the causal mutation. Thus, this study of patients harboring unreported mtDNA variants will be useful in a clinical situation. Of these, the m.14439G>A (*MT-ND6*) variant was experimentally confirmed to be a novel causative mtDNA mutation, while 1356A>G (*12S rRNA*) was confirmed to be non-pathogenic by a cybrid assay. The remaining four novel variants have yet to be experimentally elucidated, but m.5537A>G (*mt-tRNA trp*) in Pt004 is likely to be causative because m.5537AinsT was reported to be disease causing.[16]

ND6 is an mtDNA-encoded complex I subunit that is essential for the assembly of complex I and the maintenance of its structure.[17–19] *ND6* mutations were previ-

